Scheme I

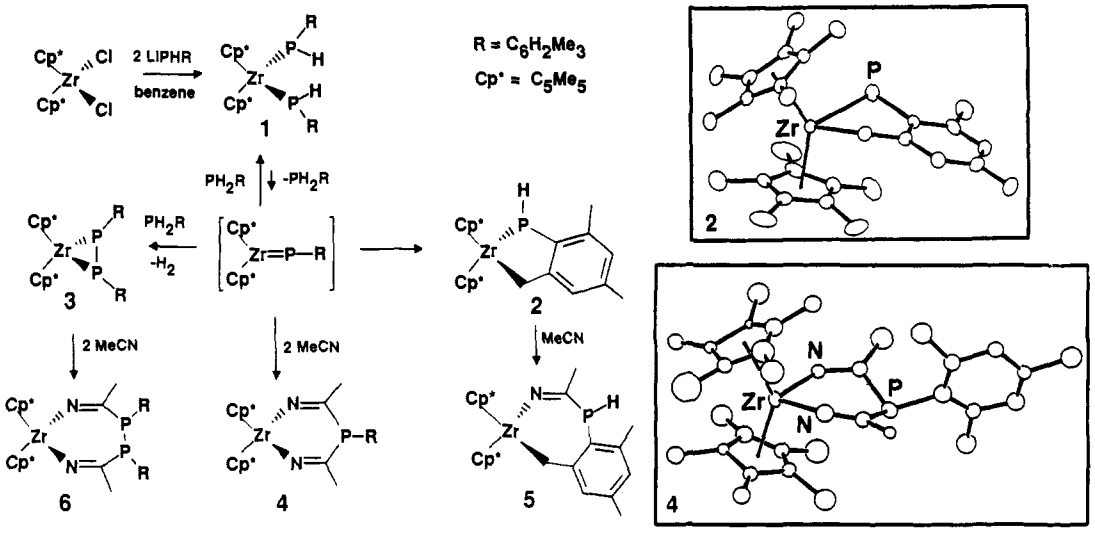

axis of symmetry with a Zr-P bond length of 2.63 (2) Å, which is typical of pyramidal phosphides on Zr(IV).

Compound **1** is a synthon for the highly reactive phosphinidene intermediate $Cp^*_2Zr{=}P(C_6H_2Me_3)$ as judged by its subsequent trapped products. Monitoring of a benzene solution of **1** by ^{31}P NMR showed the slow loss of the resonance attributable to **1** and the growth of signals attributable to two new Zr complexes, free primary phosphine $PH_2(C_6H_2Me_3)$, and traces of $(PH(C_6H_2Me_3))_2$. The new Zr complexes were isolated by fractional crystallization. After 2 days, red-brown crystals of **2** were deposited. The NMR spectra[13] and crystallographic data[13] confirmed **2** as the phosphametallocycle $Cp^*_2Zr(CH_2C_6H_2Me_2PH)$. Upon further standing for several days, a second new Zr derivative, $Cp^*_2Zr(PC_6H_2Me_3)_2$ (**3**), was obtained.[13]

Bergman et al.[2] have described the generation of $Cp_2Zr{=}NR$ from $Cp_2Zr(NHR)_2$. In our case, a similar equilibrium between **1** and the highly reactive phosphinidene intermediate accounts for the conversion of **1** to **2** and **3**. Intramolecular C-H bond activation of an *o*-methyl group in the transient phosphinidene accounts for the formation of **2**. Formation of **3** requires addition of the P-H bond of the primary phosphine to the Zr=P double bond with the opposite regiochemistry to that which permits re-formation of **1**. This yields a P-P bond, and subsequent elimination of H_2 drives the irreversible formation of **3**. Compound **2** is stable in solution, even in the presence of excess phosphine ($PH_2(C_6H_2Me_3)$) and is thus not involved in the formation of **3**. Interception of the transient phosphinidene was achieved via the reaction of a solution of **1** with MeCN in benzene at 25 °C. The products include free primary phosphine PRH_2 as well as the yellow-orange six-membered metallocycle $Cp^*_2Zr(NCMe)_2P(C_6H_2Me_3)$ (**4**).[13,14] The geometry at the phosphorus atom in **4** is pseudopyramidal. Mechanistically, this reaction may be viewed as a 2 + 2 cycloaddition of MeCN to the phosphinidene with subsequent insertion of a second equivalent of acetonitrile into the Zr-P bond. Attempts to observe the initial cycloaddition product led only to the observation of **1**, **4**, and free phosphine. Although attempts to isolate the phosphinidene intermediate have been unsuccessful to date, direct spectroscopic evidence for a phosphinidene species is derived from the reaction of LiPH($C_6H_2Me_3$) and $Cp^*_2ZrCl_2$ in DME at 25 °C. In addition to **1**, a ^{31}P NMR resonance at 537 ppm with no P-H coupling is seen. This downfield resonance is attributed to the unstable bent phosphinidene intermediate.[12c,d] Addition of MeCN to this DME solution led to the disappearance of both the resonance at 537 and that from **1** and the appearance of the signal from **4**. Attempts to trap this species employing dative donors such as PMe_3 were unsuccessful, affording instead mixtures of **2** and **3**.

It was also found that reactions of **2** and **3** with MeCN give quantitatively the seven-membered metallocycles $Cp^*_2Zr(CH_2C_6H_2Me_2PH(C(Me)N))$ (**5**) and $Cp^*_2Zr(NC(Me)P(C_6H_2Me_3))_2$ (**6**), respectively.[13]

The chemistry described herein illustrates that generation of a reactive phosphinidene intermediate offers a route to a variety of new phosphametallocycles and thus a point of entry for metal-mediated organophosphorus chemistry.

Acknowledgment. The financial support from NSERC of Canada is gratefully acknowledged.

Supplementary Material Available: Tables of crystallographic data, thermal and hydrogen atom parameters, and selected bond distances and angles for **1**, **2**, **4**, and **6** (33 pages); listing of observed and calculated structure factors for **1**, **2**, **4**, and **6** (40 pages). Ordering information is given on any current masthead page.

(14) Crystal data, **1**: $C_{38}H_{54}P_2Zr$, *Pbcn*, a = 10.941 (4) Å, b = 15.719 (6) Å, c = 21.047 (9) Å. **2**: $C_{29}H_{41}PZr$, $P2_1/n$, a = 11.724 (8) Å, b = 15.613 (6) Å, c = 14.791 (3) Å, β = 102.81 (3)°. **4**: $C_{33}H_{47}N_2PZr$, *Pbca*, n = 23.328 (6) Å, b = 18.777 (5) Å, c = 14.583 (6) Å. **6**: $C_{42}H_{58}N_2P_2Zr$, *Cc*, a = 16.722 (33) Å, b = 14.003 (3) Å, c = 17.652 (9) Å, β = 104.04 (9)°. Mo Kα radiation, λ = 0.71069 Å, and a Rigaku AFC6-S diffractometer were employed to collect the data (4.5° < 2θ < 50°). The solutions were obtained and refined employing the TEXSAN software package from MSC. Refinement (data $I > 3\sigma(I)$, variables R, R_w), **1**: 309, 55, 0.0962, 0.0967. **2**: 2740, 280, 0.0480, 0.0554. **4**: 916, 111, 0.0857, 0.0850. **6**: 1570, 212, 0.0411, 0.0482.

Is the Structure of Selenoformamide Similar to Those of Formamide and Thioformamide?

Jerzy Leszczyński,* Józef S. Kwiatkowski,*,† and Danuta Leszczyńska

Department of Chemistry
Jackson State University
Jackson, Mississippi 39217

Received April 15, 1992

Formamide and its thio and seleno analogs can formally exist in two tautomeric forms, **1** and **2** (Chart I). However, it is experimentally well documented that the amide form **1** of both formamide (F) and thioformamide (SF) is a dominating species in the vapor phase, an inert environment, and a polar medium.[1]

† Permanent address: Instytut Fizyki, Uniwersytet M. Kopernika, 87-100 Toruń, Poland.

0002-7863/92/1514-10089$03.00/0

Chart I

1 **2**

F	X = O	FA
SF	X = S	SFA
SeF	X = Se	SeFA

Unfortunately, the experimental data for selenoformamide are not available.

In the case of formamide, the experimental evidence is confirmed by the recent ab initio post-Hartree–Fock calculations[2,3] concluding that the internal energy of F at 0 K is lower by 50 kJ/mol than the energy of FA. As we shall see later, the sulfur substitution for oxygen decreases the relative internal energy of the two tautomers **1** and **2** by 10 kJ/mol, but the SF form of thioformamide still has significantly lower energy (by 40 kJ/mol) than its SFA form. It might appears that, for selenoformamide, the SeF tautomer also should dominate over the SeFA form. We shall present some arguments suggesting that such is not the case.

To predict molecular structures and properties of the title species, the ab initio post-Hartree–Fock calculations were carried out for their **1** and **2** tautomers using the Gaussian 90 program.[4] The computations were performed at the electron correlation MP2 level[5,6] with the partially uncontracted [43111/43111/4*] valence triple-ζ Huzinaga basis set for Se[7] and Dunning–Huzinaga valence double-ζ basis set for other atoms.[8] This basis set was augmented by the p and 6d polarization functions on hydrogen and heavy atoms, respectively (DTZP basis set). Full geometry optimizations were followed by the calculations of the vibrational harmonic wavenumbers. The amide forms of both thio- and selenoformamide (SF, SeF) and all three acidic forms (FA, SFA, SeFA) are predicted to be planar systems, while for the F form the calculations suggest a small deviation of the amino group from the plane containing the HC=O residue.[9]

The relative internal energies at 0 K for **1** and **2** forms of the title compounds were calculated as a sum of the relative electronic energies (the SCF energies corrected by the electron correlation contributions) and zero-point vibrational energies (ZPEs). The electron correlation contributions to the electronic energies were calculated up to full-fourth-order MP4(SDTQ)[5,6] using the DTZP basis set. Though usually the electron correlation contributions are calculated at the frozen-core (fc) approximation, we additionally performed calculations without this constraint (full electron calculations).[10] The temperature-dependent thermodynamic contributions to the Gibbs free energies of tautomerization were calculated within the rigid-rotor harmonic-oscillator ideal gas approximation[11] using the calculated rotational constants and harmonic frequencies.

Table I. Relative Energies (kJ/mol) and Relative Thermodynamic Contributions to the Gibbs Free Energies (kJ/mol) in the Gas Phase[a]

	F–FA	SF–SFA	SeF–SeFA
ΔE^{el}			
SCF[b]	53.7	56.4	51.4
CISD	50.0 (50.4)[c]	48.3 (47.6)[c]	−18.4 (27.6)[c]
MP2	51.4 (51.8)	55.9 (55.2)	−21.3 (31.2)
MP3	43.2 (43.6)	48.7 (48.2)	−29.0 (26.4)
MP4(SDQ)	48.7 (49.1)	47.8 (47.2)	−30.1 (25.4)
MP4(SDTQ)	50.3 (50.6)	50.8 (50.0)	−30.7 (25.1)
ΔZPE	2.0[d]	−8.7	−10.6
$\Delta H(0)$[e]	52.3 (52.6)	42.1 (41.3)	−41.3 (14.5)
$\int_0^T \Delta C_p\, dT$	2.0	−0.3	−0.1
$-T\Delta S$	−5.0	0.5	0.1
$\Delta G(T) - \Delta G(0)$	−3.0	0.2	0.0

[a] All data calculated at the MP2/DTZP optimized geometries. [b] The SCF/DTZP energies (in au): F, −168.974 15; SF, −491.190 99; SeF, −2491.820 92. [c] Calculated with the frozen-core (fc) approximation. [d] Calculated at the MP2/6-31G** level, ref 3. [e] The relative internal energies at 0 K ($\Delta E^{SCF} + \Delta E^{MP4(SDTQ)} + \Delta$ZPE). The internal energies with $\Delta E^{MP4(SDTQ)}$ calculated within the fc approximation are given in parentheses.

Table II. Energies of the Core MOs (au) of SeF and SeFA and Their Relative MP2 Energies (kJ/mol) vs the Number of "Frozen" MOs

core MOs[a]	E_{MO}[b] SeF	E_{MO}[b] SeFA	no. of frozen MOs	ΔE^{MP2}
12–16 Se(3d)	−2.60	−2.66	16 (fc)	31.2
9–11 Se(3p)	−6.62	−6.69	11	29.3
8 Se(3s)	−8.89	−8.96		
7 C(1s)	−11.36	−11.33	7	27.7
6 N(1s)	−15.63	−15.57		
3–5 Se(2p)	−54.27	−54.34	5	−20.8
2 Se(2s)	−60.65	−60.71	2	−21.1
1 Se(1s)	−460.29	−460.36	0 (full)	−21.3

[a] The major contributions of AOs to the MOs are given in parentheses. [b] Approximate MO energies.

The predicted relative stability of F–FA tautomers (Table I) is not very sensitive to the level of calculations (except the calculations at the MP3 level). In the case of SF–SFA species the difference between SCF and MP4(SDTQ) relative energies amounts to 5.6 kJ/mol. For both F–FA and SF–SFA pairs, the relative electron correlation energies calculated with full electron calculations and within fc approximations differ at most by 0.8 kJ/mol. Quite surprising data were obtained for the SeF–SeFA pair. Though at the SCF level the relative energy of SeF–SeFA species is similar to those of the F–FA and SF–SFA pairs, inclusion of the electron correlation contributions at the fc approximations stabilizes the SeFA form by 20–26 kJ/mol (this effect depends only slightly upon the order of perturbation theory). Inclusion of the electron correlation for both core and valence electrons stabilizes SeFA by an additional 56 kJ/mol (MP4(SDTQ)), reversing the stability pattern observed for the F–FA and SF–SFA pairs. Also ZPE contributions decrease additionally the relative energy of SeFA by 10.6 kJ/mol, resulting in −41.3 kJ/mol, our best prediction of its relative internal energy at 0 K. Temperature dependent thermodynamical contributions are negligible for the selenoformamide tautomers.

To determine which orbitals are responsible for the unusual properties of selenoformamide, a number of calculations were carried out at the MP2 level incorporating different core MOs in computations of the electron correlation contributions (Table

(1) For instance, see: (a) Hirota, E.; Sugisaki, R.; *J. Mol. Spectrosc.* **1974**, *49*, 251. (b) Brown, R. D.; Godfrey, P. D.; Kleinbomer, B. *J. Mol. Spectrosc.* **1987**, *124*, 34. (c) Ladell, J.; Post, B. *Acta Crystallogr.* **1954**, *7*, 559. (d) Ottersen, T. *Acta Chem. Scand.* **1975**, *A29*, 939. (e) Räsanen, M. *J. Mol. Struct.* **1983**, *101*, 245. (f) Sugisaki, R.; Tanaka, T.; Hirota, E. *J. Mol. Spectrosc.* **1974**, *49*, 241.

(2) (a) Wang, X.-Ch.; Nichols, J.; Feyereisen, M.; Gutowski, M.; Boatz, J.; Haymet, A. D.; Simons, J. *J. Phys. Chem.* **1991**, *95*, 10419. (b) Wong, M. W.; Wiberg, K. B.; Frisch, M. J. *J. Am. Chem. Soc.* **1992**, *114*, 1645.

(3) Kwiatkowski, J. S.; Leszczyński, J. *J. Mol. Struct.* **1992**, *270*, 67.

(4) GAUSSIAN 90, Revision H. Frisch, M. J.; Head-Gordon, M.; Trucks, G. W.; Foresman, J. B.; Schlegel, H. B.; Raghavachari, K.; Robb, M.; Binkley, J. S.; Gonzalez, C.; Melius, S. F.; Baker, J.; Martin, S. F.; Kahn, L. R.; Stewart, J. J. P.; Topiol, S.; Pople, J. A. Gaussian Inc., Pittsburgh, PA, 1990.

(5) Møller, C.; Plesset, M. S. *Phys. Rev.* **1934**, *46*, 618.

(6) Hehre, W. H.; Radom, L.; Schleyer, P. v. R.; Pople, J. A. *Ab Initio Molecular Orbital Theory*; Wiley: New York, 1986.

(7) Huzinaga, S.; Andzelm, J.; Klobukowski, M.; Radzio-Andzelm, E.; Sakai, Y.; Tatewaki, H. *Gaussian Basis Sets for Molecular Orbital Calculations*; Elsevier: New York, 1977.

(8) (a) Dunning, T. H. *J. Chem. Phys.* **1970**, *53*, 2823. (b) Dunning, T. H.; Hay, P. J. In *Modern Theoretical Chemistry*; Schaefer, H. F., III, Ed.; Plenum Press: New York, 1977; Vol. 3, p 1.

(9) The MP2/6-31G** calculations show that the nonplanar form of F is lower than the planar structure by only 0.003 kJ/mol (for details see ref 3).

(10) The frozen-core (fc) option used by default in the GAUSSIAN 90 program does not select correctly the frozen core for molecules with a selenium atom (the fc option does not freeze the 3d electrons!). We have used the ReadWindow option to select the proper orbitals to be frozen.

(11) McQuarrie, D. *Statistical Mechanics*; Harper and Row: New York, 1986.

II). We concluded that the sixth and seventh MOs consisting predominantly of the N(1s) and C(1s) AOs are crucial for the relative stability of the SeFA tautomer. As is evident from the presented data, its relative energy decreases monotonically upon increasing the number of MOs included in the MP2 calculations; however, inclusion of the sixth and seventh MOs drops the ΔE^{MP2} energy from +27.7 to -20.8 kJ/mol.

As one can see, the electron correlation effects are essential in prediction of the relative electronic energies of the studied selenium compounds, and some trends are evident (the shift of the **1** ⇄ **2** equilibrium upon oxygen substitution by sulfur and selenium). In this respect, the present study is the first example of ab initio quantum-mechanical calculations at the electron correlation level that noticed and explained unexpected properties of selenium in systems that mimic simple units of biologically important structures. The predicted differences in the tautomeric equilibria of selenoformamide compared with oxo- and thioformamide might be of importance in explanations of the role of the selenium atom in such biological systems as, for example, selenoproteins.

The following important conclusions emerge from this investigation:

1. Contrary to the formamide and thioformamide cases, the selenoformimidic acid (SeFA) is the lowest energy species. Predicted energy differences (Table I) suggests that SeFA should be observed in the gas phase and/or inert gas matrices, and perhaps this form should exist exclusively in neutral environments.

2. The calculated dipole moments of SeF and SeFA (4.43 and 1.48 D, respectively) show that the tautomeric equilibrium between SeF and SeFA should be shifted toward SeF on going from the gas phase to a polar medium.

3. As is evident from the presented data, the theoretical studies of tautomeric (isomeric) equilibria of the systems involving fourth-row (or heavier) elements should be carried out at the correlated level including both valence and core electrons. It seems that when MP4(full) calculations are not affordable, it is more appropriate to compare MP2(full) rather than MP4(fc) relative energies.

Acknowledgment. We gratefully acknowledge Grant DAAL03-89-0038 from the Army High Performance Computing Research Center. We also thank the Mississippi Center for Supercomputing for an allotment of computer time for the calculations presented here.

Supplementary Material Available: Table III containing calculated molecular parameters including bond lengths and bond angles, dipole moments, rotational constants, and SCF and MP2 energies for selenoformamide and selenoformimidic acid (1 page). Ordering information is given on any current masthead page.

Apparent Endo-Mode Cyclic Carbopalladation with Inversion of Alkene Configuration via Exo-Mode Cyclization–Cyclopropanation–Rearrangement

Zbyslaw Owczarczyk, Frédéric Lamaty, Edward J. Vawter, and Ei-ichi Negishi*

Department of Chemistry, Purdue University West Lafayette, Indiana 47907

Received July 20, 1992

We recently documented what appeared to be the first reported example of cyclopropanation of neopentyl-type alkylpalladium species.[1,2] Since it could compete with common ring formation in cases where cascade carbopalladation[3] involves the addition of alkenylpalladium species to 1,1-disubstituted alkenes, we undertook to dilineate its scope. The cyclic versions of the process mentioned above may be classified into the two types shown in Scheme I, according to the substrate structure. The exo-mode cyclization process is arbitrarily shown.

Scheme I

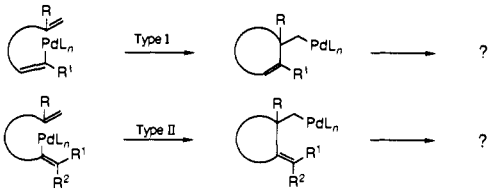

As the results summarized in Scheme II indicate, cyclopropanation via carbopalladation of neopentyl-type alkylpalladium species appears to be a generally observable process with the type I substrates in the absence of a faster or competitive process, such as common ring formation, provided that there is a β-hydrogen syn-coplanar with Pd in the putative (cyclopropylcarbinyl)palladium intermediates.

In sharp contrast, the type II reaction has predominantly yielded apparent endo-mode cyclization products. Typically, treatment of **1**[4] with 3% of $PdCl_2(PPh_3)_2$, 20% of Et_2NH, and NEt_3 in DMF at 80 °C for 8 h provided **2**[5] in 69% yield. It is significant to note that the reaction proceeded with complete inversion of the alkene configuration. The stereochemistry of **2** was established by ^1H 2D NOESY NMR spectroscopy. Consequently, a mechanism involving a straightforward endo-mode carbopalladation of **3** to give **4** must be ruled out. Such a process would proceed with retention of alkene configuration.

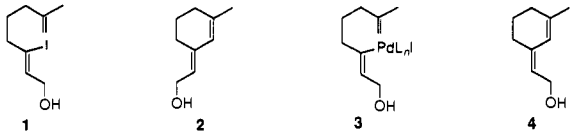

1 2 3 4

More consistent not only with the observed stereochemistry but also with the results of the type I cyclization reactions is a sequence involving (i) exo-mode carbopalladation, (ii) cyclopropanation, and (iii) cyclopropylcarbinyl-to-homoallyl rearrangement (Scheme III). We believe that the experimental results and literature information presented below fully support this mechanism, which unifies the mechanisms of the type I and type II reactions.

Since the plausibility of the mechanism shown in Scheme III critically hinges on the stereochemistry of the reaction, all products containing a stereodefined exocyclic alkene moiety have been subjected to ^1H 2D NOESY NMR spectroscopic analysis. All such products, i.e., **2** and **5–9**,[5] yielded NMR spectroscopic data confirming inversion of alkene configuration shown in Scheme III. The *E* configuration of **5** was further established by X-ray analysis of its *p*-nitrobenzoate. Conversion of **10**[4] into **5** in 68% yield was carried out as that of **1** into **2**. The same procedure was also satisfactory for converting **11**[6] into **6** in 94% yield, while the reaction of enynes, e.g., **12**[7] and **13**,[7] with organic halides, e.g., PhI and α-bromostyrene, catalyzed by Pd–phosphine complexes, e.g., $Pd(PPh_3)_4$, provides a convenient procedure for the type II

(1) Zhang, Y.; Negishi, E. *J. Am. Chem. Soc.* **1989**, *111*, 3454.

(2) For subsequent reports on this subject, see: (a) Grigg, R.; Dorrity, M. J.; Malone, J. F.; Sridharan, V.; Sukirthalingam, S. *Tetrahedron Lett.* **1990**, *31*, 1343. (b) Grigg, R.; Sridharan, V.; Sukirthalingam, S. *Tetrahedron Lett.* **1991**, *32*, 3855. (c) Meyer, F. E.; Parsons, P. J.; de Meijere, A. *J. Org. Chem.* **1991**, *56*, 6487. For a related cyclobutanation, see: Carpenter, N. E.; Kucera, D. J.; Overman, L. E. *J. Org. Chem.* **1989**, *54*, 5896.

(3) For a review, see: Negishi, E. *Pure Appl. Chem.* **1992**, *64*, 323. See also: Zhang, Y.; Wu, G.; Agnel, G.; Negishi, E. *J. Am. Chem. Soc.* **1990**, *112*, 8590.

(4) Prepared by treatment of the corresponding propargyl alcohols with $LiAlH_4$ and NaOMe followed by iodinolysis (Corey, E. J.; Katzenellenbogen, J. A.; Posner, G. H. *J. Am. Chem. Soc.* **1967**, *89*, 4245).

(5) All cyclization products have been identified by spectroscopic methods including high-resolution mass spectroscopy.

0002-7863/92/1514-10091$03.00/0